

# Pharmacological Targeting of Glucagon and Glucagon-Like Peptide 1 Receptors Has Different Effects on Energy State and Glucose Homeostasis in Diet-Induced Obese Mice<sup>[S]</sup>

Wei Gu, David J. Lloyd, Narumol Chinookswong, Renée Komorowski, Glenn Sivits Jr., Melissa Graham, Katherine A. Winters, Hai Yan, Laszlo G. Boros, Richard A. Lindberg, and Murielle M. Véniant

*Departments of Metabolic Disorders (W.G., D.J.L., N.C., R.K., G.S., M.G., K.A.W., R.A.L., M.M.V.) and Protein Sciences (H.Y.), Amgen Inc., Thousand Oaks, California; and SiDMAP, LLC, Los Angeles, California (L.G.B.)*

Received January 26, 2011; accepted March 28, 2011

## ABSTRACT

Pharmacologic contributions of directly agonizing glucagon-like peptide 1 (GLP-1) receptor or antagonizing glucagon receptor (GCGR) on energy state and glucose homeostasis were assessed in diet-induced obese (DIO) mice. Metabolic rate and respiratory quotient (RQ), hyperglycemic clamp, stable isotope-based dynamic metabolic profiling (SiDMAP) studies of <sup>13</sup>C-labeled glucose during glucose tolerance test (GTT) and gene expression were assessed in cohorts of DIO mice after a single administration of GLP-1 analog [GLP-1-(23)] or anti-GCGR antibody (Ab). GLP-1-(23) and GCGR Ab similarly improved GTT. GLP-1-(23) decreased food intake and body weight trended lower. GCGR Ab modestly decreased food intake without significant effect on body weight. GLP-1-(23) and GCGR Ab decreased RQ with GLP-1, causing a greater effect. In a hyperglycemic clamp, GLP-1-(23) reduced hepatic glucose

production (HGP), increased glucose infusion rate (GIR), increased glucose uptake in brown adipose tissue, and increased whole-body glucose turnover, glycolysis, and rate of glycogen synthesis. GCGR Ab slightly decreased HGP, increased GIR, and increased glucose uptake in the heart. SiDMAP showed that GLP-1-(23) and GCGR Ab increased <sup>13</sup>C lactate labeling from glucose, indicating that liver, muscle, and other organs were involved in the rapid disposal of glucose from plasma. GCGR Ab and GLP-1-(23) caused different changes in mRNA expression levels of glucose- and lipid metabolism-associated genes. The effect of GLP-1-(23) on energy state and glucose homeostasis was greater than GCGR Ab. Although GCGR antagonism is associated with increased circulating levels of GLP-1, most GLP-1-(23)-associated pharmacologic effects are more pronounced than GCGR Ab.

## Introduction

Agonizing the glucagon-like peptide 1 (GLP-1) receptor (GLP-1R) and antagonizing the glucagon receptor (GCGR) are two therapeutic approaches for achieving improved glycemic control. In preclinical animal models both GLP-1R agonists and GCGR antagonists exhibit robust efficacy in lowering blood glucose levels (Wang et al., 1997; Greig et al., 1999; Liang et al., 2004; Yan et al., 2009). Although the two hormones control distinct pathways in regulating glucose production and dis-

posal, studies have demonstrated that the two approaches are interdependent in achieving maximal therapeutic efficacy (Gu et al., 2009). It has been demonstrated that the glucose-lowering effects of GLP-1 are mediated by multiple activities, including enhancement of glucose-stimulated insulin secretion (Drucker et al., 1987),  $\beta$ -cell preservation (Xu et al., 1999), and inhibition of gastric emptying (Wettergren et al., 1993; Nauck et al., 1997). GLP-1 also enhances satiety and decreases energy intake (Flint et al., 1998; Näslund et al., 1999). It has been proposed that GLP-1 lowers fasting blood glucose by suppressing glucagon secretion (Drucker and Nauck, 2006). Conversely, both mice and cynomolgus monkeys treated with GCGR antagonist displayed compensatory elevations of active GLP-1 levels (Yan et al., 2009).

Article, publication date, and citation information can be found at <http://jpet.aspetjournals.org>.  
doi:10.1124/jpet.111.179986.

[S] The online version of this article (available at <http://jpet.aspetjournals.org>) contains supplemental material.

**ABBREVIATIONS:** GLP-1, glucagon-like peptide 1; GLP-1R, GLP-1 receptor; GCGR, glucagon receptor; SiDMAP, stable isotope-based dynamic metabolic profiling; HGP, hepatic glucose production; DIO, diet-induced obese; Ab, antibody; GTT, glucose tolerance test; ipGTT, intraperitoneal GTT; RQ, respiratory quotient; PBS, phosphate-buffered saline; 2-[<sup>14</sup>C]DG, 2-deoxy-D-[1-<sup>14</sup>C] glucose; TCA, tricarboxylic acid; WAT, white adipose tissue; BAT, brown adipose tissue; G6PDH, glucose-6-phosphate dehydrogenase; Pepck, phosphoenolpyruvate carboxykinase; PkI<sub>r</sub>, pyruvate kinase; PEG, polyethylene glycol.

We have demonstrated that the antidiabetic effects of GCGR antagonism depended on GLP-1R agonism and were not just associated with enhanced GLP-1 levels (Gu et al., 2010). Using two independent experimental approaches, GLP-1R antagonism and genetic loss of GLP-1R function, we demonstrated that complete efficacy of a GCGR antagonist requires a functional GLP-1 receptor. These findings, however, do not imply that GLP-1 agonists and GCGR antagonists have identical effects on all aspects of glucose homeostasis. The two agents may have distinct effects on energy and glucose metabolism.

GLP-1 decreases body weight in humans and animal models (Meeran et al., 1999; Zander et al., 2002; Raun et al., 2007), and glucagon has hypolipemic effects that include inhibition of hepatic lipogenesis and stimulation of ketogenesis (Unger and Orci, 1975; Klain, 1977; Reed et al., 1984). In light of the roles of GLP-1 and glucagon, it is not surprising that GLP-1R agonists and GCGR antagonists have overlapping and contrasting effects on the overall metabolic state. In the studies reported here, we investigated the pharmacologic contributions of directly agonizing the GLP-1 receptor or antagonizing GCGR on energy state and glucose homeostasis in diet-induced obese (DIO) mice. To gain molecular insight on the mechanisms of action, we conducted metabolomic analysis using stable isotope-based dynamic metabolic profiling (SiDMAP) and transcriptional analysis of key metabolic pathways in treated DIO mice. Our data indicate that the two agents exhibit differential effects on energy metabolism and certain aspects of glucose homeostasis in a DIO rodent model. These data contribute to an understanding of the benefits and limitations of these two therapeutic agents.

## Materials and Methods

**Experimental Animals.** All mouse studies were conducted at Amgen Inc. and were performed in accordance with guidelines and regulations approved by the Institutional Animal Care and Use Committee. The use of radioactive material in animals was approved under the guidelines of the Amgen radiation safety committee. Mice were maintained on a 12-h light/dark cycle with free access to food and water. Administration of test articles was performed between 7:00 AM and 9:00 AM on ad libitum-fed animals. Three-week-old male C57BL/6 mice were obtained from Charles River Laboratories, Inc. (Wilmington, MA). After 12 to 22 weeks of either a standard diet (Harlan Teklad, Madison, WI) or a high-fat diet (D12492; Research Diets, Inc., New Brunswick, NJ), mice were stratified on the basis of fed plasma glucose levels and body weight and were randomly assigned to a treatment group.

**Generation and Characterization of Anti-GCGR and GLP-1 Analog.** The generation and characterization of the anti-GCGR antibody used in all of the experiments have been described previously (Yan et al., 2009). In brief, GCGR Ab is a human monoclonal IgG that antagonizes GCGR. In cells expressing recombinant mouse GCGR, GCGR Ab inhibited glucagon-induced cAMP elevation ( $IC_{50} \sim 1.8$  nM). The generation of the GLP-1 analog has been described previously (Miranda et al., 2008). As shown by Miranda et al., GLP-1 compound **5** was PEGylated with a C-terminal cysteine-alanine extension to give GLP-1 compound **23** ( $EC_{50} \sim 0.13$  nM). Compound **23** was used in every study and is abbreviated as GLP-1-(23).

**GLP-1 and GCGR Ab Effects on Glucose Tolerance Test in DIO Mice.** Three groups of 20- to 22-week-old male mice fed a high-fat diet for 16 to 18 weeks were sorted on the basis of plasma glucose and body weight into groups having similar distributions. These mice were injected intraperitoneally with either vehicle, GLP-1-(23), or GCGR Ab at 10  $\mu$ g/mouse or 1 mg/kg/body weight, respec-

tively, 24 h before the ipGTT was initiated. Mice were fasted for 12 h (9:00 PM to 9:00 AM), and a fasted plasma glucose measurement was taken at  $\sim$ 9:00 AM (time 0 or GTT baseline) for each mouse. Mice were injected intraperitoneally with D-glucose (2 g/3.33 ml/kg body weight); plasma glucose levels were measured with a hand-held glucometer at 30 and 90 min after the glucose bolus injection (AlphaTrak; Abbott Laboratories, Abbott Park, IL) from blood that had been sampled retro-orbitally in nonanesthetized mice. Terminal blood collection was obtained at 120 min after glucose bolus for plasma hormone analysis.

**Metabolic Rate and Activity.** DIO mice were prepared as described previously (Xu et al., 2009) and acclimated to the metabolic rate cages for 16 days before analysis. Metabolic rate was assessed with the Comprehensive Laboratory Animal Monitoring System (Columbus Instruments, Columbus, OH). Data on  $O_2$  consumption ( $VO_2$ ; ml/kg/h),  $CO_2$  production ( $VCO_2$ ; ml/kg/h), and activity (beam breaks) were collected every 20 min for 7 days. Respiratory quotient (RQ) was derived from the ratio of  $VCO_2$  to  $VO_2$ . Daily body weight and food intake were manually measured. Stable baseline values were collected for 24 h before injection with test articles.

**Hyperglycemic Clamp.** The 19-week-old male C57BL/6 mice (Charles River Laboratories) studied were fed a high-fat diet for 15 weeks ( $n = 21$ ). Mice were catheterized at least 4 days before the *in vivo* experiments after being anesthetized under isoflurane (3%) in oxygen. A silastic catheter (0.025 o.d.) connected with Micro Renathane (MRE 0.025) was inserted in the right jugular vein. The free catheter end was tunneled under the skin to the back of the neck and sealed with a stainless-steel plug. Lines were flushed daily with  $\sim$ 50  $\mu$ l of saline containing 100 units/ml heparin and 5 mg/ml ampicillin. Mice were treated with either PBS (vehicle) for 24 h, GLP-1-(23) at 10  $\mu$ g/mouse for 24 h, or GCGR Ab at 1 mg/kg for 72 h before the hyperglycemic clamp procedure. Compound doses and maximal efficacy were determined in a separate pilot study, and the clamp procedure was initiated when maximal efficacy was obtained (data not shown). On the day of the clamp experiment, a three-way connector was attached to the jugular vein catheter for intravenous infusion. Mice were maintained in a Plexiglas mouse restrainer (mice had been acclimated for 2 h per day for 2 days before the clamp procedure). After a 12-h overnight fast, and 2 h before initiating the clamp procedure, [ $3\text{-}^3\text{H}$ ] glucose (PerkinElmer Life and Analytical Sciences, Waltham, MA) was infused continuously (0.05  $\mu$ Ci/min). The [ $3\text{-}^3\text{H}$ ] glucose preinfusion began at 7:00 AM ( $t = -120$  to 0 min) followed by 2 h of [ $3\text{-}^3\text{H}$ ] glucose infusion at 0.1  $\mu$ Ci/min. Blood samples (20  $\mu$ l) from the tip of the tail were collected at 20-min intervals for the immediate measurement of plasma glucose levels, and 20% glucose was infused at variable rates to maintain hyperglycemia between 250 and 300 mg/dl. All infusions were performed by using a pump (Harvard Apparatus Inc., Holliston, MA). To estimate glucose uptake in individual tissues, 2-deoxy-D-[1- $^{14}\text{C}$ ] glucose (2-[ $^{14}\text{C}$ ]DG; PerkinElmer Life and Analytical Sciences) was administered as a bolus (10  $\mu$ l) 75 min after the start of the clamp. Blood samples were taken before, during, and at the end of the infusion for measurement of plasma [ $^3\text{H}$ ]glucose,  $^3\text{H}_2\text{O}$ , 2-[ $^{14}\text{C}$ ]DG concentrations, and/or insulin concentrations. At the end of the procedure, tissues (brain, gastrocnemius, white and brown adipose, liver, heart, stomach, duodenum, jejunum, and ileum) were taken for biochemical analysis.

**Biochemical Assays.** Glucose concentrations during clamps were analyzed by using 10  $\mu$ l of plasma with the glucose oxidase method and the glucose analyzer GM9D (Analox Instruments, Lunenburg, MA). Plasma insulin concentrations from the hyperglycemic clamp study were measured by enzyme-linked immunosorbent assay (Crystal Chem Inc., Downers Grove, IL) following the manufacturer's instructions. The Milliplex Kit MENDO-75K (Millipore Corporation, Billerica, MA) was used according to the manufacturer's protocol to measure plasma insulin, active GLP-1, and glucagon. A standard curve of GLP-1-(23) was used to quantify this species

at a dilution of plasma in which endogenous active GLP-1 levels were undetectable.

[3-<sup>3</sup>H] Glucose, <sup>3</sup>H<sub>2</sub>O, and 2-[<sup>14</sup>C] DG plasma samples were deproteinized with Ba(OH)<sub>2</sub> and ZnSO<sub>4</sub> and then immediately centrifuged. An aliquot from each supernatant was counted directly with a LS6500 liquid scintillation counter (Beckman Coulter, Fullerton, CA) and another aliquot was dried to remove <sup>3</sup>H<sub>2</sub>O, which was determined as the difference between dried and undried samples.

Tissue samples were homogenized for determination of tissue 2-[<sup>14</sup>C] DG-6-phosphate content. Supernatants were subjected to an ion-exchange column (Bio-Rad pre-filled poly prep column 100-200; Bio-Rad Laboratories, Hercules, CA) to separate 2-[<sup>14</sup>C]DG-6-phosphate from 2-[<sup>14</sup>C]DG.

**Injection of Stable Isotope in DIO Mice.** DIO mice (prepared as described previously) were injected intraperitoneally with either PBS (vehicle), GLP-1-(23) at 10 μg/mouse, or GCGR Ab at 1 mg/kg. Beginning 12 h after receiving the injection, mice were fasted for 12 h. Mice were bled from the retro-orbital sinus for baseline blood glucose measurement 24 h after injection of PBS, GLP-1-(23), or GCGR Ab. After the baseline blood glucose levels were measured, mice were injected intraperitoneally with uniformly labeled <sup>13</sup>C glucose tracer ([U-<sup>13</sup>C<sub>6</sub>]-D-glucose; 2 g/kg), which was purchased from Sigma-Aldrich-Isotec Isotope Laboratories (Miamisburg, OH) and had >98% isotopic purity and >99% positional accuracy. Thirty minutes after the tracer injection, mice were bled via the retro-orbital sinus. At 90 min after tracer injection, mice were decapitated, blood was collected, and liver, skeletal muscle (gastrocnemius/soleus), kidney, and white adipose tissues (WAT; epididymal) were removed. As samples were harvested, all were flash-frozen in liquid nitrogen and stored at -80°C until SiDMAP analysis.

**SiDMAP Analysis.** In vivo metabolism of [U-<sup>13</sup>C<sub>6</sub>]-D-glucose produces several stable, nonradiating isotope-labeled intermediary metabolite species, also called mass isotopomers. Among these isotopomer products  $m_1$  has one <sup>13</sup>C substitution;  $m_2$  has two and  $m_n$  has  $n$  <sup>13</sup>C substitutions at the corresponding carbon positions (Boros et al., 2002). These isotopomers were readily separated and measured by using gas chromatography/mass spectrometry techniques described below and elsewhere (Leimer et al., 1977; Lee et al., 1995, 1998; Wahl et al., 2010).

**<sup>13</sup>C Metabolite Isotopomer Profile Analyses.** Absorption of <sup>13</sup>C glucose was monitored by the clearance of the  $m_6$  <sup>13</sup>C isotopomer from plasma, and hepatic TCA cycle activity was monitored by the reappearance of the  $m_1$  isotopomer of glucose. Blood plasma (20 μl) was deproteinized and deionized, and the derived glucose was treated with hydroxylamine hydrochloride in pyridine and acetic anhydride to create the aldonitrile penta-acetate derivative for gas chromatography/mass spectrometry analysis. The glucose fragment with carbons 1 to 4 and its positional isotopomers were monitored at the  $m/z$  242 ion cluster.

Lactate was used for the measurement of label incorporation into the three-carbon metabolite pool during anaerobic glycolysis. Lactate from the plasma (20 μl) was extracted by ethyl acetate after acidification with HCl. Lactate was derivatized to its propylamine-heptafluoro-butyl ester form, and the  $m/z$  328 (carbons 1–3 of lactate, chemical ionization) was monitored for the detection of  $m_2$  (recycled lactate through the pentose cycle) and  $m_3$  (lactate produced by the Embden-Meyerhof-Parnas pathway) for the estimation of glucose-triose cycling in control and drug-treated animals (Lee et al., 1998).

**Glutamate.** Glutamate label distribution from glucose is used for discriminating glucose oxidation from anabolic glucose use within the TCA cycle, a process called anaplerotic flux (Lee et al., 1996). To obtain glutamate, plasma (20 μl) was first treated with 6% perchloric acid. The supernatant was passed through a 3-cm<sup>3</sup> Dowex-50 (H<sup>+</sup>) column. Amino acids were eluted with 15 ml of 2 N ammonium hydroxide. To further separate glutamate from glutamine, the amino acid mixture was passed through a 3-cm<sup>3</sup> Dowex-1 (acetate) column and then collected with 15 ml of 0.5 N acetic acid. The dry glutamate fraction from the plasma was converted to its trifluoroacetyl butyl

ester (Leimer et al., 1977). Under EI conditions, ionization of trifluoroacetyl butyl ester-glutamate gives rise to two fragments,  $m/z$  198 and  $m/z$  152, corresponding to C<sub>2</sub>-C<sub>5</sub> and C<sub>2</sub>-C<sub>4</sub> of glutamate. Glutamate labeled on the 4 and 5 carbon positions indicates pyruvate dehydrogenase activity, whereas glutamate labeled on the 2 and 3 carbon positions indicates pyruvate carboxylase activity for the re-entry of glucose carbons to the TCA cycle. TCA cycle anabolic glucose utilization is calculated by using the  $m_1/m_2$  ratios of glutamate (Lee et al., 1996).

**CO<sub>2</sub>.** Tissues having a wet weight of 100 mg were homogenized in 1 ml of distilled water, from which 100 μl was removed and treated with 0.1 N HCl and NaHCO<sub>3</sub> to release HCO<sub>3</sub>-bound and dissolved CO<sub>2</sub> to determine <sup>13</sup>CO<sub>2</sub>/<sup>12</sup>CO<sub>2</sub> ratios. Released <sup>12</sup>CO<sub>2</sub> was monitored at  $m/z$  44 and <sup>13</sup>CO<sub>2</sub> was monitored at  $m/z$  45 in the electron impact ionization mode.

**Gas Chromatography/Mass Spectrometry.** Mass spectral data were obtained on the HP5975N mass selective detector connected to an HP6890N gas chromatograph (Hewlett Packard, Palo Alto, CA). The settings were as follows: GC inlet 230°C, transfer line 280°C, MS source 230°C, MS Quad 150°C. An HP-5 capillary column (30 m length, 250 μm diameter, 0.25 μm film thickness) was used for glucose, lactate, and glutamate analysis.

**Gene Expression Analysis.** Livers were removed 90 min after injection of the stable isotope from the mice described under *Injection of Stable Isotope in DIO Mice*.

They were then frozen in liquid nitrogen and stored at -80°C until processed. Livers were homogenized in the Tissuelyser (Qiagen, Valencia, CA), and total RNA was extracted from the lysate using the RNeasy Plus Mini system (Qiagen). All protocols were followed according to the manufacturer's instructions. Quantitative real-time polymerase chain reaction was performed on the ABI Prism 7900HT Sequence Detection System using One-Step RT-PCR Master Mix Reagents (Roche Molecular Systems Inc., Branchburg, NJ) according to the manufacturer's instructions and using the primer sets listed in Table 1. Samples were analyzed in quadruplicate and normalized to mouse cyclophilin-A (NM\_008907).

**Statistical Analysis.** Statistical analyses were performed using StatView 5.0.1 (SAS Institute, Cary, NC) or Prism version 5.0 (GraphPad Software Inc., San Diego, CA) analysis of variance for multiple comparisons. Mass spectral analyses were performed using three independent automatic injections of 2-μl samples by the automatic sampler and accepted only if the standard sample deviation was less than 1% of the normalized peak intensity. Statistical analysis was performed using the parametric unpaired, two-tailed independent sample *t* test with 99% confidence intervals ( $\mu \pm 2.58 \sigma$ ).  $P < 0.05$  was considered to indicate significant differences in glucose carbon metabolism in plasma and organs in comparison with the control group.

## Results

### GLP-1-(23) and GCGR Ab Similarly Improved ipGTT.

To determine whether antagonizing the glucagon pathway and activating the GLP-1 pathway would similarly improve glucose tolerance in DIO mice, vehicle, GLP-1-(23), or GCGR Ab were administered 24 h before an ipGTT. Doses and maximal efficacy were determined in separate pilot studies. Mice were sorted into three groups so the mean glucose levels and body weight were not significantly different from one another (Fig. 1A, sorting prebleed). Sorting body weight were  $48 \pm 1$ ,  $48 \pm 1$ , and  $49 \pm 1$  g for the vehicle, GLP-1-(23), and GCGR Ab groups, respectively. Fasting plasma glucose levels were measured to determine GTT baseline (Fig. 1A). In mice treated with GLP-1-(23), fasting plasma glucose levels were significantly decreased compared with those of vehicle-treated mice. Glucose tolerance was similarly improved by

TABLE 1  
Primer sets used

	Forward	Reverse	Probe
Gys2	GCA CGG AGA GGC TCT CAG AT	AGG TGT CTG GCA TGC TGG TAA	TC CTG GAC TGG AGA TAC CTG GGC AGA
PGC1a	AGT GAA GAT GAA AGT GAT AAA CTG AGC T	GAA GGC GAC ACA TCG AAC AA	TT GGG ATG GCA CGC AGC CCT ATT
Gck	TTT ATG ACC CCC GCT AGT CCT	CGT GCC TGT GAA AGC GTG T	CA CTC GCG CCG CCC ACA TG
G6pc	GAA AGA AAA AGC CAA CGT ATG GA	GCA CAG CCC AGA ATC CCA	CC ACA AGA TGA CGT TCA AAC ACC GGA
G6pd	TTT GGC CCC ATC TGG AAT C	CCC CCA CGA CCC TCA GTA C	AT TGC TTG TGT GAT CCT CAC ATT TAA AGA GCC
Pygl	CCA TTT ACC AGC TTG GAT TGG A	CCC AAG ACC GCC ATT GC	AA GGC CCG CAT CTT CTT CAA TTT CTT CTA ACT CT
PKLR	GGA CCG CCT CAA GGA GAT G	TGG GAG CCA TGG GAG AAG T	GA GTC GTG CAA TGT TCA TCC CTG CCT
Fbp1	CTG CAT GTT GTA CAT TCC TAG AAA CA	TTG GGC ATT GCA AAG CAT TA	CC TAA CAG CGT GGA TAG TTT CAC AGC
HNFa	CCG GGC TGG CAT GAA G	GAC CTC CGC GTG CTG ATC	TC CCG CTC ATT TTG GAC AGC TTC CT
Pepck	ATC CAG GGC AGC CTC GA	AGC ATT GCC TTC CAC GAA CT	AG CCT GCC CCA GGC AGT GAG G
ACC2	TGC ATG GGA TGC TGA TCA AT	TGT GCC TGG AAT CGC TTA GC	CG CCC TAT GTC ACC AAG GAC CTG CT
ACADm	CAA GTT TGC CAG AGA GGA GAT TAT C	AAC GGG TAC TCC CCG CTT T	CC GTC GCC CCG GAA TAT GAC
ACAD1	CGA GAA GTT CAT CCC CCA GAT	CCA GGC TCT GTC ATG GCT ATG	CA CCG ATA CAC TTG CCC GCC G
CPT1a	GAT ACA CCA ACG GGC TCA TCT T	CAA AAT GAC CTA GCC TTC TAT CGA AT	CC CAC CCA GTC AGA TTC CAA CCA GAG
ACOX1	CCT TCA CTT GGG CAT GTT CCT	GAA ACG CTC CTG CTG CTC TT	CC CAC CTT GCT TCA CCA GGC CA
PPARa	ACG ATG CTG TCC TCC TTG ATG	GTG TGA TAA AGC CAT TGC CGT	CG CGA TCA GCA TCC CGT CTT TGT
BDH1	TAG CGG CCA CCA GTC TCT ACA	CAG GTC ATC CCA CAT CTT CTT G	CC GAG CGC ATC CAG GCC ATC
HMGCS2	GCT ACT GGG ATG GTC GCT ATG	GGC GTT ACC ACT CGG GTA GA	AA TGT CAC CAC AGA CCA CCA GG
SREBP1c	GGA GCC ATG GAT TGC ACA TT	TCA AAT AGG CCA GGG AAG TCA	AA GAC ATG CTT CAG CTT ATC AAC AAC CAA GAC A
SREBP1a	GCC GAG ATG TGC GAA CTG	GTC ACT GTC TTG GTT GTT GAT GAG	AC AGC GGT TTT GAA CGA CAT CGA AGA C
CD36	GAT TTG TTC TTC CAG CCA ATG C	TCA GTG CAG AAA CAA TGG TTG TC	TT GCA TCA CCC CTC CAG AAT CC
ABCB4	CCC AGG AAC CCA TTC TCT TTG	ACC CGG CTG TTG TCT CCA TA	TG CAG CAT CGC AGA GAA CAT CGC
ABCD2	CCA TAG CAA CCG TGG AGG TAA	CCA CAT CAA TAA CTG TTC CTT TGA TG	CT GGA ACT ACC CCT CAG CGA CAC CC
UCP2	TCA CTG TGC CCT TAC CAT GCT	AGG CAT GAA CCC CTT GTA GAA G	CG CGG GGT CCC TCC TTC CG
Murine cyclophilin2	CAA ATG CTG GAC CAA ACA CAA	GCC TTC TTT CAC CTT CCC AAA	TT CCC AGT TTT TTA TCT GCA CTG CCA AGA

Gys2, glycogen synthase 2; PGC1a, peroxisome proliferator-activated receptor  $\gamma$  coactivator 1 $\alpha$ ; Gck, glucokinase; G6pc, glucose-6-phosphatase, catalytic; G6pd, glucose-6-phosphate dehydrogenase; Pygl, phosphorylase glycogen liver; PKLR, red cell pyruvate kinase; Fbp1, fructose 1,6 biphosphatase; HNFA, hepatocyte nuclear factor 4 $\alpha$ ; ACC2, acetyl CoA-carboxylase 2; ACADm, acyl-CoA dehydrogenase, C-4 to C-12 straight chain; ACAD1, Acyl-CoA dehydrogenase, long chain; CPT1a, carnitine palmitoyltransferase 1A; ACOX1, acyl-CoA oxidase; PPARa, peroxisome proliferator-activated receptor  $\alpha$ ; BDH1, 3-hydroxybutyrate dehydrogenase, type 1; HMGCS2, 3-hydroxy-3-methylglutaryl-CoA synthase 2; SREBP1c, sterol-regulatory-element-binding protein-1c; SREBP1a, sterol-regulatory-element-binding protein-1a; CD36, cluster of differentiation 36; ABCB4, ATP-binding cassette B4; ABCD2, ATP-binding cassette D2; UCP2, uncoupling protein 2.

both treatments (Fig. 1B). A terminal bleed at 120 min was used to measure plasma hormone levels. GCGR Ab was the only treatment that significantly decreased insulin levels (Fig. 1C). We collected enough blood to measure glucose levels but not enough to be able to measure insulin levels at time points earlier than 120 min. We have measured insulin levels during ipGTT in previous studies and have shown that, as expected, insulin levels were increased at 15 min (Gu et al., 2010). Endogenous active GLP-1 levels were increased in GCGR Ab-treated mice (Fig. 1D), whereas pharmacological levels of active GLP-1 were detected in the plasma of GLP-1-(23)-treated mice. Compared with glucagon levels in mice treated with vehicle, glucagon levels were significantly increased in mice treated with GCGR Ab (Fig. 1E), whereas plasma glucagon levels were significantly decreased in mice treated with GLP-1-(23).

**GLP-1-(23) and GCGR Ab Exhibit Differential Effects on Metabolic Rate and Respiratory Quotient.** To test the effects of inhibiting the GCGR pathway or activating the GLP-1 receptor pathway on metabolic rate and RQ, three groups of DIO mice were treated with vehicle, GLP-1-(23), or GCGR Ab. As expected, treatment with GLP-1-(23) significantly reduced food intake and moderately reduced body weight in DIO mice, whereas GCGR Ab-treated mice exhibited a more modest, yet significant, reduction in food intake

without a change in body weight (Fig. 2, A and B). A biphasic circadian rhythm of O<sub>2</sub> consumption typical for the nocturnal habits of rodents was observed. Immediately after injection of GLP-1-(23) or GCGR Ab significant decreases in O<sub>2</sub> consumption and CO<sub>2</sub> production were observed in the DIO mice (Fig. 2, C and D). GLP-1-(23) affected these parameters to a greater extent than the GCGR Ab. Physical activity of the GLP-1-(23)-treated mice declined, whereas it was unchanged by GCGR Ab (Fig. 2E). It is noteworthy that the respiratory quotient was greatly decreased with GLP-1-(23) treatment but only slightly decreased with the GCGR Ab (Fig. 2F). These effects were sustained for approximately 60 h after the administration of each treatment and demonstrated marked return to pretreatment levels. A rebound effect was observed on RQ in mice treated with GLP-1-(23) but not in mice treated with GCGR Ab.

**Hyperglycemic Clamp in DIO Mice Treated with GLP-1-(23) or GCGR Ab.** A 2-h hyperglycemic clamp combined with intravenous administration of [3-<sup>3</sup>H]glucose and [1-<sup>14</sup>C]2-deoxyglucose was performed in mice fed a high-fat diet for 15 weeks and treated with GLP-1-(23) or vehicle 24 h before initiating the procedure. GCGR Ab was administered 72 h before the hyperglycemic clamp because we have shown previously that after this period of time glucose levels were maximally decreased (Yan et al., 2009). The basal (12-h over-

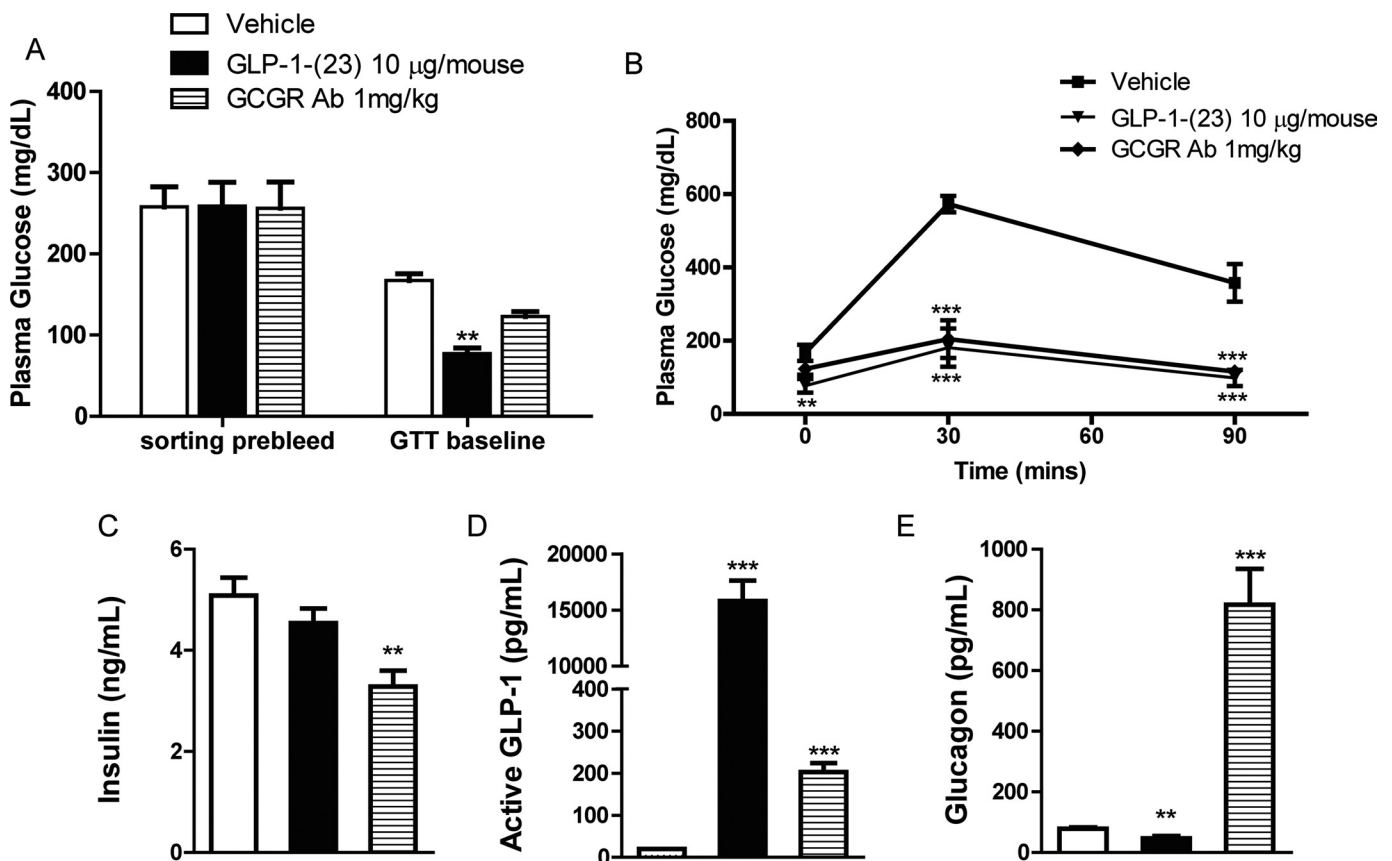


**Fig. 1.** GLP-1(23) and GCGR Ab similarly improved glucose tolerance in DIO mice. A, mice were sorted on plasma glucose (sorting prebleed). Fasting plasma glucose was measured after a 12-h fast, initiated 12 h after vehicle, GLP-1(23) at 10 µg/mouse, or GCGR Ab at 1 mg/kg had been administered (GTT baseline). B, ipGTT was initiated 24 h after the drug treatment. Plasma glucose was measured in mice fasted for 12 h. Mice were then injected intraperitoneally with 2 g/kg glucose solution, and plasma glucose levels were again measured at 30 and 90 min after glucose injection. Mice were treated with vehicle (■), GLP-1(23) (▼), or GCGR Ab (●). C to E, blood was collected 120 min after glucose bolus to measure plasma insulin (C), active GLP-1 (D), and glucagon (E) levels. All data are means ± S.E.M ( $n = 6-7$  per group). \*\*,  $P < 0.01$ ; \*\*\*,  $P < 0.001$  versus vehicle-treated, high-fat diet-fed mice.

night fast) and clamp glucose and insulin levels are shown in Fig. 3, A and B. Basal plasma glucose levels were decreased to a greater extent with GLP-1(23) than with GCGR Ab (Fig. 3A). The clamped plasma glucose selection criterion that was targeted for each animal ranged from 250 to 300 mg/dl. Mice that did not reach the plasma glucose target range were excluded from the study. Compared with vehicle-treated or GCGR Ab-treated mice, a larger number of mice treated with GLP-1(23) demonstrated clamped glucose levels near 300 mg/dl, causing this group to be significantly increased compared with the other groups. As expected, basal and clamped insulin values only showed significant increases in mice treated with GLP-1(23) (Fig. 3B). The glucose infusion rate required to maintain hyperglycemia (250–300 mg/dl) was approximately 70- and 24-fold higher in the GLP-1(23) and GCGR Ab-treated mice, respectively, than in vehicle-treated mice (Fig. 3C). The basal hepatic glucose production (HGP) was not altered by a single dose of GCGR Ab or GLP-1(23) treatment (Fig. 3D). However, the clamped hepatic glucose production rate was significantly reduced by 45% in GCGR Ab-treated mice, whereas it was completely reversed in GLP-1(23)-treated mice (Fig. 3D) to favor glucose uptake.

**Glucose Turnover Rates and Glucose Utilization by Tissues in DIO Mice Treated with GLP-1(23) or GCGR Ab.** Whole-body glucose turnover and glycolysis were significantly elevated in mice treated with either GLP-1(23) or

GCGR Ab (Fig. 4). Only GLP-1(23), however, significantly increased the rate of glucose storage as glycogen or lipid synthesis (Fig. 4). The [ $^{14}\text{C}$ ]2-DG uptake was measured in the stomach and different parts of the intestine (Fig. 5A). Glucose uptake was significantly decreased in the jejunum, but not in the duodenum or ileum, in mice treated with either GLP-1(23) or GCGR Ab. The major action of GLP-1 is thought to be mediated by regulation of pancreatic hormones. However, GLP-1R mRNAs have been found in multiple tissues including brain, kidney, heart, fat, skeletal muscle, liver, and intestine (Egan et al., 1994). Whether the suppression of glucose uptake in the intestine is mediated directly by the GLP-1R signaling remains to be further investigated. In the other measured tissues, only brown adipose or heart (for GCGR Ab only) showed significant increases in glucose uptake in mice treated with GLP-1(23) or GCGR Ab, respectively (Fig. 5, B and C).

**GCGR Ab and GLP-1(23) Decreased Circulating Glucose Levels.** Glucose can be deposited in RNA, DNA, amino acids, and fatty acids for macromolecule synthesis or recycled for energy production during an ipGTT (Leimer et al., 1977). U- $^{13}\text{C}$  glucose, in which  $^{13}\text{C}$  occupies all six carbons, is readily taken up from the plasma by tissues. Supplemental Fig. 1 highlights glucose metabolic pathways monitored in this study in various tissues. Absorption of administered glucose was monitored by the clearance of the  $m_6$   $^{13}\text{C}$  glucose isoto-

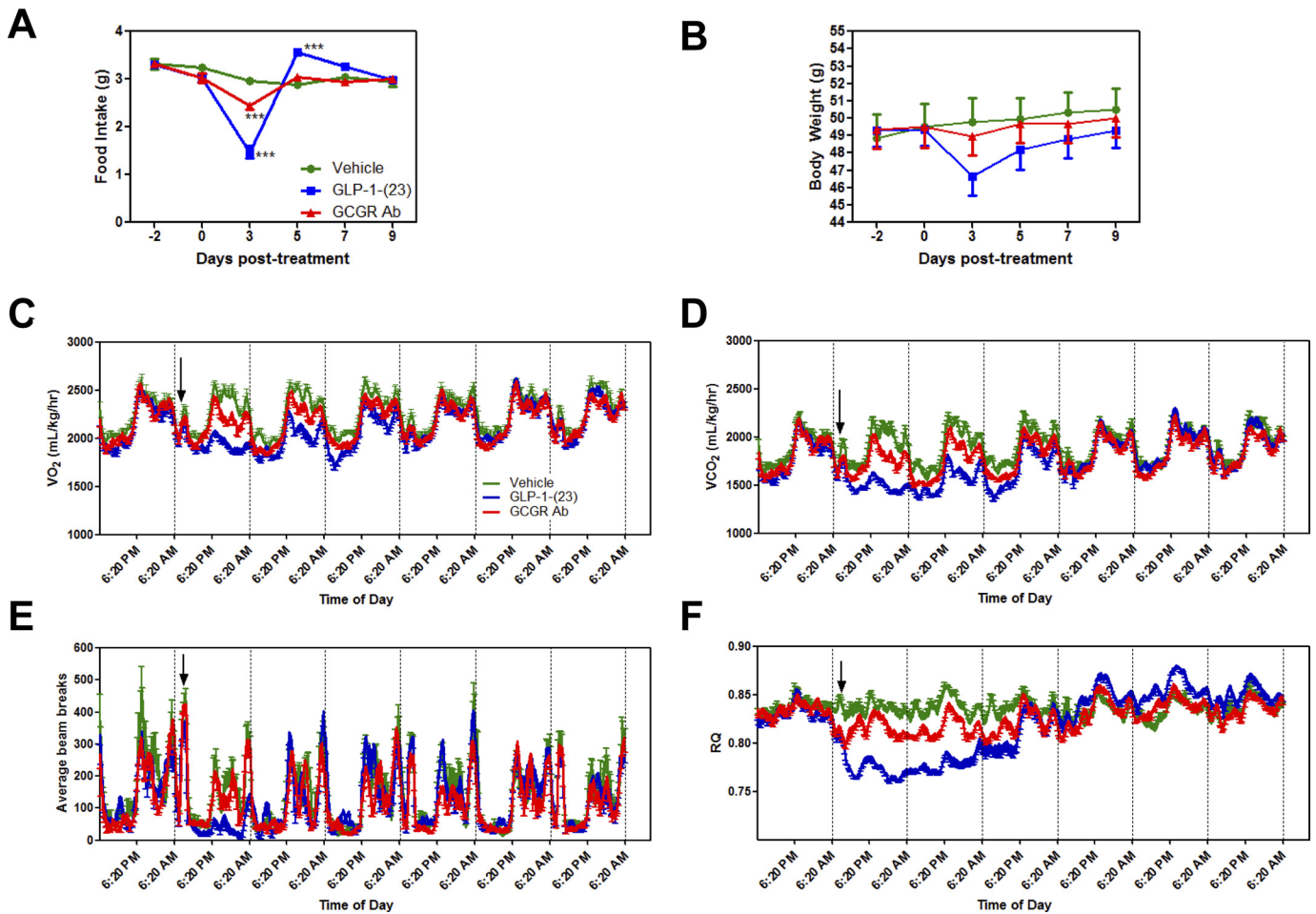


**Fig. 2.** Indirect calorimetry in mice treated with GLP-1(23) and GCGR Ab. Mice were assessed before and after treatment with either a single injection of GLP-1(23) (blue), GCGR Ab (red), or vehicle (green),  $n = 6, 7, 8$ , respectively. Time of injection is indicated by the vertical arrows. Food intake (A), body weight (B), oxygen consumption ( $VO_2$ ) (C),  $CO_2$  production ( $VCO_2$ ) (D), physical activity (E), and RQ (F) were continuously monitored. Data represent mean  $\pm$  S.E.M. \*\*\*,  $P < 0.001$  versus vehicle-treated, high fat diet-fed mice.

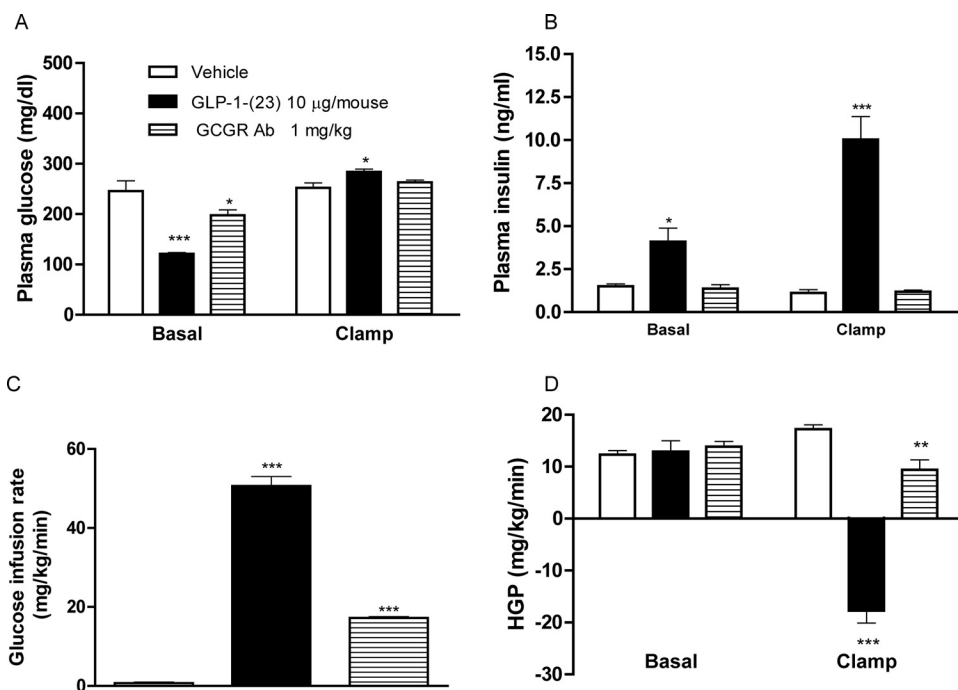


**Fig. 3.** GLP-1(23) reduces plasma glucose and increases insulin levels in DIO mice. Mice were treated with vehicle (open bars), GLP-1(23) (filled bars), or GCGR Ab (striped bars) intraperitoneally at doses of 0 (vehicle), 10  $\mu$ g/mouse, or 1 mg/kg, respectively. Mice were fasted for 12 h, and blood was collected at basal and during the hyperglycemic clamp conditions. A, plasma glucose levels during basal and clamp conditions. B, plasma insulin levels during basal and clamp conditions. C, glucose infusion rate. D, basal rates of HGP and, glucose-stimulated rates of HGP during clamps. All data are means  $\pm$  S.E.M. ( $n = 6-7$ ). \*,  $P < 0.05$ ; \*\*,  $P < 0.01$ ; \*\*\*,  $P < 0.001$  versus vehicle-treated mice.

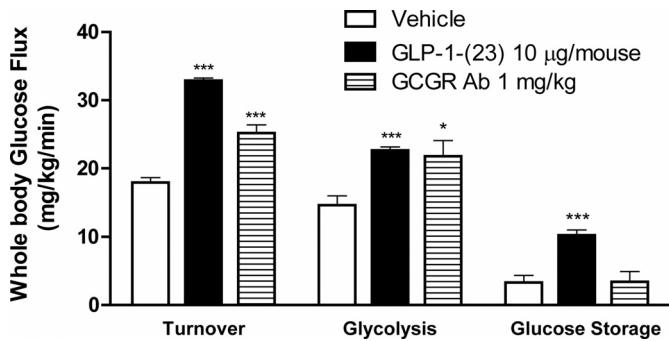


**Fig. 4.** GLP-1-(23) and GCGR Ab improved whole-body glucose metabolism. Left, whole-body glucose turnover. Center, whole-body glycolysis. Right, whole-body glucose metabolite storage. All data are means  $\pm$  S.E.M. ( $n = 6-7$ ). \*,  $P < 0.05$ ; \*\*\*,  $P < 0.001$  versus vehicle-treated mice.

pomer from plasma, and hepatic TCA cycle activity was monitored by the appearance of the  $m_1$  isotopomer of glucose. Injection of 2 g/kg of uniformly labeled  $^{13}\text{C}_1$ - $^{13}\text{C}_4$ -labeled glucose via the intraperitoneal route resulted in a significant increase in the  $m_1$  isotopomer of glucose in plasma above the 500 mg/dl range, as seen in control animals treated with vehicle at 30 min ( $526 \pm 19.6$  mg/dl; Fig. 6A). This level persisted for at least 90 min ( $578 \pm 21.6$  mg/dl, Fig. 6A). GLP-1-(23) treatment prevented the rapid increase in blood glucose  $m_1$  isotopomer levels observed in the vehicle-treated animals at 30 min. Levels of this isotopomer reached  $148 \pm 7.9$  mg/dl at 30 min and  $167 \pm 11.6$  mg/dl at 90 min. The reduction of the appearance of the  $m_1$  isotopomer in plasma glucose at 30 and 90 min was less pronounced with GCGR Ab treatment than with GLP-1-23 ( $380 \pm 69.3$  and  $303 \pm 16.13$  mg/dl at respective time points).

**GCGR-Ab and GLP-1-(23) Induced Intensely Labeled Plasma Lactate from  $^{13}\text{C}$  Glucose Tracer.** Lactate is the main three-carbon product of glycolysis and is readily secreted into the plasma. Therefore, lactate was used for the measurement of label incorporation into the three-carbon metabolite pool during anaerobic glycolysis. The possible ar-

rangements of  $^{13}\text{C}$  labels from  $[\text{U}-^{13}\text{C}_6]$ -D-glucose to lactate are  $[\text{U}-^{13}\text{C}_3]$ -lactate produced by glycolysis and  $[2,3-^{13}\text{C}_2]$ -lactate produced by direct glucose oxidation in the pentose cycle and recycling. It has been shown that the isotopomers of lactate are the products of isotopomers of glucose and the contribution from pyruvate kinase (Pklr) recycling of lactate via the TCA cycle is minimal (Lee et al., 1998).

Animals treated with vehicle metabolized the injected labeled glucose into labeled circulating lactate to  $15.9 \pm 0.7$  and  $29.0 \pm 1.2\%$  of total lactate by 30 and 90 min, respectively (Fig. 6B). At 30 min, animals treated with GCGR Ab showed a greater percentage of total lactate labeled with  $^{13}\text{C}$  relative to vehicle-treated control animals (Fig. 6B). Animals treated with GLP-1-(23) rapidly metabolized  $^{13}\text{C}$  glucose to plasma lactate by 30 min with nearly no further increase in percentage of total lactate labeling between 30 and 90 min (Fig. 6B). This rapid increase in  $^{13}\text{C}$  lactate labeling from glucose indicated that glycolysis in liver and muscle, as well as other organs, was partially responsible for the rapid disposal of glucose from the plasma (Lee et al., 1998).

**Plasma Glutamic Acid  $^{13}\text{C}$  Labeling Is Indicative of Increased TCA Cycle Flux and Citrate Shuttling after GCGR Ab and GLP-1-(23) Treatments.** The TCA cycle and cytoplasmic metabolite  $\alpha$ -ketoglutarate is in close equilibrium with glutamate, which is readily released by mammalian mitochondria into the cytosol and then into the plasma. Glutamate label distribution from glucose is suitable for determining glucose oxidation versus anabolic glucose use within the cycle, also known as anaplerotic flux (Lee et al., 1996). On one hand,  $^{13}\text{C}$  labeling in C1, C2, and C3 (but not C4 and C5) of glutamate represents the terminal oxidation of an unlabeled substrate, i.e. high rates of fatty acid derived acetyl-CoA oxidation. On the other hand, glutamate labeled with  $^{13}\text{C}$  on C4 and C5 indicates tracer glucose-derived acetyl-CoA oxidation. Glutamate labeled on the 4 and 5 carbon positions indicates pyruvate dehydrogenase activity, whereas glutamate labeled on the 2 and 3 carbon positions

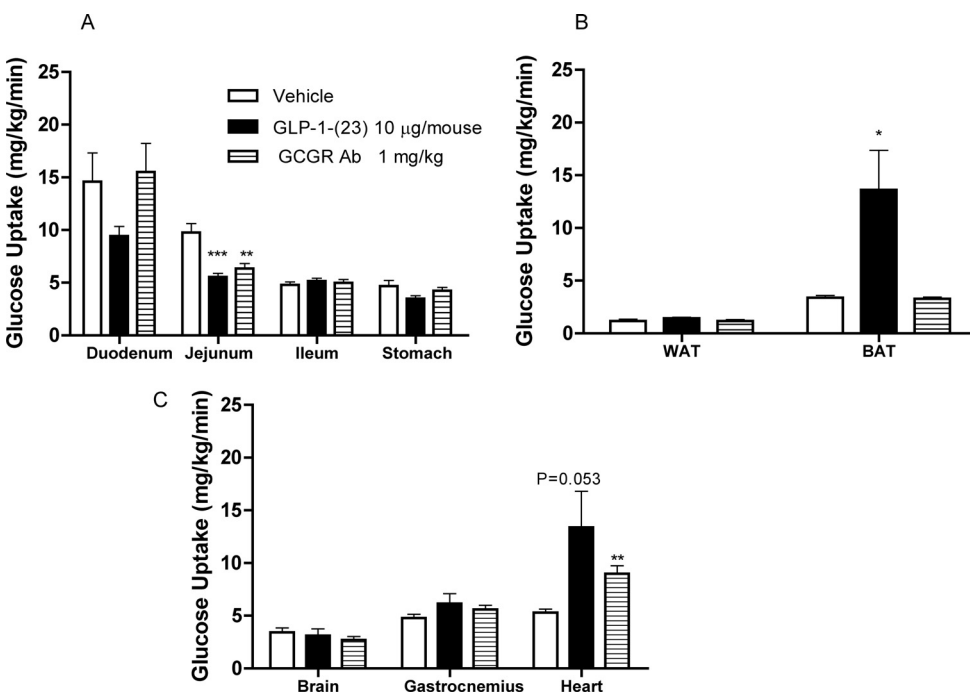


**Fig. 5.** GLP-1-(23) and GCGR Ab improve tissue-specific glucose uptake in DIO mice. Glucose uptake in individual organs during the clamp procedure was assessed using 2- $^{14}\text{C}$ deoxyglucose uptake assay on DIO mice treated with vehicle (open bars), GLP-1-(23) (filled bars), or GCGR Ab (striped bars). Glucose uptake is shown for duodenum, jejunum, ileum, and stomach (A), WAT and BAT (B), and brain, gastrocnemius, and heart (C). All data are means  $\pm$  S.E.M. ( $n = 6-7$ ). \*,  $P < 0.05$ ; \*\*,  $P < 0.01$ ; \*\*\*,  $P < 0.001$  versus vehicle-treated.

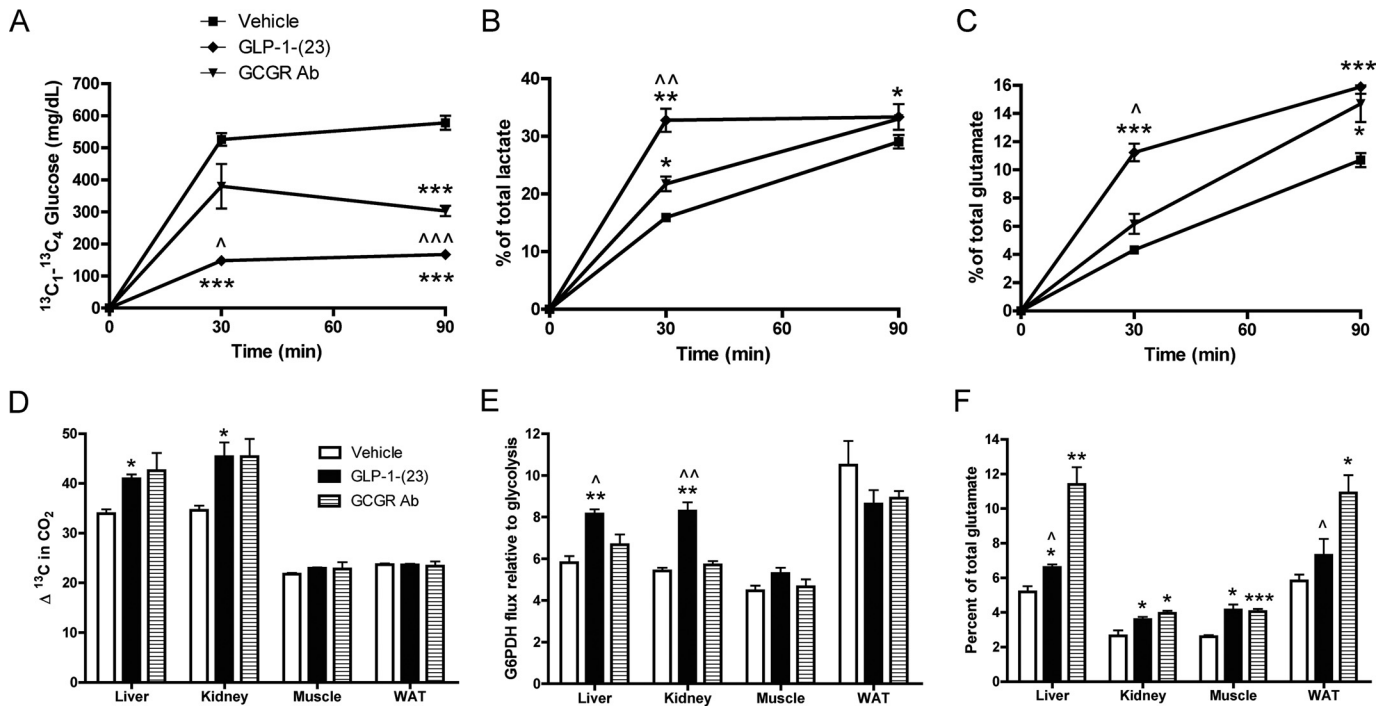


**Fig. 6.** In vivo metabolism of  $[\text{U-}^{13}\text{C}_6]$ -D-glucose produces several stable, nonradiating isotope-labeled intermediary metabolite species, also called mass isotopomers. DIO mice were injected with either PBS (vehicle), GLP-1-(23) at  $10 \mu\text{g}/\text{mouse}$ , or GCGR Ab at  $1 \text{ mg}/\text{kg}$ . Twenty-four hours after the treatment was initiated and 12 h after a fast, mice were injected intraperitoneally with uniformly labeled  $^{13}\text{C}$  glucose tracer ( $[\text{U-}^{13}\text{C}_6]$ -D-glucose;  $2 \text{ g}/\text{kg}$ ). A, blood was collected from the mice at time 0 (before the glucose bolus), and after 30 and 90 min for measurement of  $\text{U-}^{13}\text{C}_6$ -glucose-derived  $m_1$  mass isotopomer  $^{13}\text{C}_1\text{-}^{13}\text{C}_4$ -glucose production. B, percentage of  $^{13}\text{C}$ -labeled plasma lactate. C, percentage of  $^{13}\text{C}$ -labeled plasma glutamate determinations. At 90 min after tracer injection, mice were decapitated and liver, skeletal muscle (gastrocnemius/soleus), kidney, and WAT (epididymis) were removed. D to F,  $^{13}\text{C}$ -labeled  $\text{CO}_2$  (D), G6PDH flux (E), and glutamate (F) were measured in these tissues. All data are means  $\pm$  S.E.M. ( $n = 6\text{--}7$ ). \*,  $P < 0.05$ ; \*\*,  $P < 0.01$ ; \*\*\*,  $P < 0.001$  versus vehicle-treated.  $\wedge$ ,  $P < 0.05$ ;  $\wedge$ ,  $P < 0.01$  versus GCGR Ab.

indicates pyruvate carboxylase activity for the re-entry of glucose carbons to the TCA cycle.

Thirty and 90 min after glucose tracer administration, animals treated with vehicle generated circulating  $^{13}\text{C}$  glutamate at  $4.33 \pm 0.65$  and  $10.7 \pm 0.5\%$  of the total glutamate pool, respectively (Fig. 6C), as a result of increased flux of pyruvate kinase and pyruvate dehydrogenase toward glucose disposal (Lee et al., 1996). Animals treated with GCGR Ab effectively used TCA cycle anaplerosis for glucose disposal as evidenced by the increasing introduction of newly formed glucose-derived glutamate ( $6.17 \pm 0.71\%$  at 30 min and  $14.69 \pm 1.3\%$  at 90 min) into circulation. GLP-1-(23) elicited an earlier response, generating  $11.24 \pm 0.62\%$  of newly formed plasma glutamate at 30 min and maintaining this increase to  $15.98 \pm 0.5\%$  at 90 min. These observations are indicative of citrate shuttling from mitochondria for glucose disposal after treatment with the compounds (Lee et al., 1996).

**GCGR Ab and GLP-1-(23) Increased Glucose Oxidation in the Liver and Kidneys of DIO Mice.** One hundred-milligram tissue samples of liver, kidney, muscle, and WAT from each animal were used to determine the number of carbon dioxide molecules per 1000 that were replaced by  $^{13}\text{CO}_2$  90 min after the glucose tracer had been administered (Fig. 6D). The calculated number is known as  $\Delta^{13}\text{C}$  in  $\text{CO}_2$  and corresponds to  $\text{HCO}_3^-$  initially bound and subsequently released from cells. This SiDMAP analysis allows the measurement of the rate at which complete tracer glucose oxidation in the TCA cycle takes place against the other main source for energy production, fatty acids. GCGR Ab treat-

ment only increased the number of  $^{13}\text{CO}_2$  molecules by complete tracer glucose oxidation to  $42.5 \pm 3.6$  and  $45.4 \pm 3.6 \text{ mg}/\text{dl}$  in the liver and kidneys, respectively, but not in muscle and WAT (unchanged at  $22.8 \pm 0.7$  and  $23.4 \pm 0.5 \text{ mg}/\text{dl}$  in muscle and WAT, respectively). Likewise, GLP-1-(23) treatment significantly increased  $^{13}\text{CO}_2$  release to  $40.9 \pm 0.9$  and  $45.3 \pm 2.9 \text{ mg}/\text{dl}$  in liver and kidney, respectively, but had no effect in muscle and WAT (unchanged with  $23.0 \pm 0.2$  and  $23.6 \pm 0.2 \text{ mg}/\text{dl}$  in muscle and WAT, respectively). These findings indicate that GCGR Ab and GLP-1-(23) increased liver- and kidney-specific complete glucose oxidation and that the disposal of glucose via mitochondrial  $\text{CO}_2$  release is an additional mechanism used to achieve glycemic control observed in these obese animals.

**GLP-1-(23) Increased Pentose Cycle Flux in the Liver and Kidneys.** The pentose phosphate shunt comprises an oxidative branch regulated by glucose-6-phosphate dehydrogenase (G6PDH) and a nonoxidative branch regulated by transketolase. Glucose first passes through the oxidative branch for direct oxidation by G6PDH, followed by pentose recirculation back into glycolysis via transketolase. This process leaves an isotopic mark on released lactate, from which G6PDH flux can be determined when pyruvate cycling is minimal. In liver, kidney, muscle, and WAT tissues from control animals  $6 \pm 0.31$ ,  $5 \pm 0.16$ ,  $4 \pm 0.24$ , and  $11 \pm 1.15$  glucose molecules, per 100, respectively, went through G6PDH metabolism before lactate release (Fig. 6E). This number is known as G6PDH flux relative to glycolysis and closely reflects the production of NADPH used for new fatty acid synthesis via reductive reactions of the fatty acid synthase complex. G6PDH flux relative to glycolysis was

not significantly different with GCGR monoclonal Ab treatment compared with vehicle treatment in liver, kidney, muscle, and WAT. However, GLP-1-(23) treatment significantly increased G6PDH metabolized glucose, each yielding two NADPH molecules, to  $8.2 \pm 0.2$  and  $8.3 \pm 0.4$ , respectively, in liver and the kidneys, but left it unchanged in muscle and WAT ( $5.3 \pm 0.3$  and  $8.6 \pm 0.7$ , respectively). Because the most robust use of NADPH is de novo fatty acid synthesis, it is evident that GLP-1-(23) increased reductive synthesis and net fatty acid production by increasing direct glucose oxidation in the pentose cycle.

**TCA Cycle Pyruvate Carboxylase Flux Is Increased with GCGR Ab Treatment in Liver and WAT and with GLP-1-(23) Treatment in Muscle.** The formation of glutamate from glucose involves the pyruvate carboxylase and pyruvate dehydrogenase mitochondrial enzymes, whereby ketoglutarate ( $\alpha$ ) is formed from oxaloacetate and citrate. Ketoglutarate transformation via glutamate dehydrogenase is one of the robust anaplerotic (anabolic use of glucose) markers linked with the Krebs cycle for glucose disposal, amino acid, and protein synthesis. Liver, kidney, muscle, and WAT of vehicle-treated animals generated newly formed  $^{13}\text{C}$ -labeled glutamate at  $5.2 \pm 0.3$ ,  $2.75 \pm 0.3$ ,  $2.6 \pm 0.1$ , and  $5.83 \pm 0.4\%$ , respectively (Fig. 6F). GCGR Ab approximately doubled the  $^{13}\text{C}$ -labeled glutamate fraction to  $11.4 \pm 1.0$ ,  $10.9 \pm 1.0$ , and  $4.1 \pm 0.3$  in liver, WAT, and muscle, respectively, whereas GLP-1-(23) treatment nearly doubled the  $^{13}\text{C}$ -labeled glutamate fraction to  $4.2 \pm 0.3\%$  in muscle. Isotopomer analysis of the  $^{13}\text{C}$ -labeled glutamate fraction indicated that the increase in  $^{13}\text{C}$  labeling in tissue glutamate occurred primarily via pyruvate carboxylase, which is the anaplerotic TCA cycle enzyme for glucose disposal in response to GCGR Ab treatment in liver, WAT, and muscle or that with GLP-1-(23) in muscle (Fig. 6F).

**GCGR Ab and GLP-1-(23) Treatment Altered Gene Expression Levels in Livers of DIO Mice.** Glucose-6-phosphatase, catalytic, and fructose 1,6 biphosphatase mRNA expression levels were significantly reduced by both GLP-1-(23) and GCGR Ab treatment (Fig. 7A), whereas phosphoenolpyruvate carboxykinase (Pepck) expression was reduced only by GCGR Ab treatment. GLP-1-(23) significantly reduced mRNA levels of Pklr and GCGR Ab increased expression of glucokinase. Both GLP-1-(23) and GCGR Ab treatment increased expression of G6PDH, but the increase did not reach statistical significance. Expression levels of peroxisome proliferator-activated receptor  $\alpha$ , peroxisome proliferator-activated receptor  $\gamma$  coactivator 1 $\alpha$ , acyl-coenzyme A dehydrogenase, C-4 to C-12 straight chain, and carnitine palmitoyltransferase 1A (liver) were significantly increased in GLP-1-(23)-treated mice, and sterol-regulatory-element-binding protein-1c levels were reduced (Fig. 7B). This regulation was not observed in GCGR Ab-treated mice.

## Discussion

It is remarkable that a single dose of either of the two antidiabetic agents, GLP-1 analog and GCGR antagonist Ab, exhibit very similar profiles of improved glucose excursion during ipGTT (Fig. 1B). The question remains whether the antidiabetic effects exhibited by the two agents are mediated by overlapping or distinct mechanisms of action. GLP-1R agonists improve glycemic control via multiple mechanisms. Although it is generally accepted that inhibition of the glu-

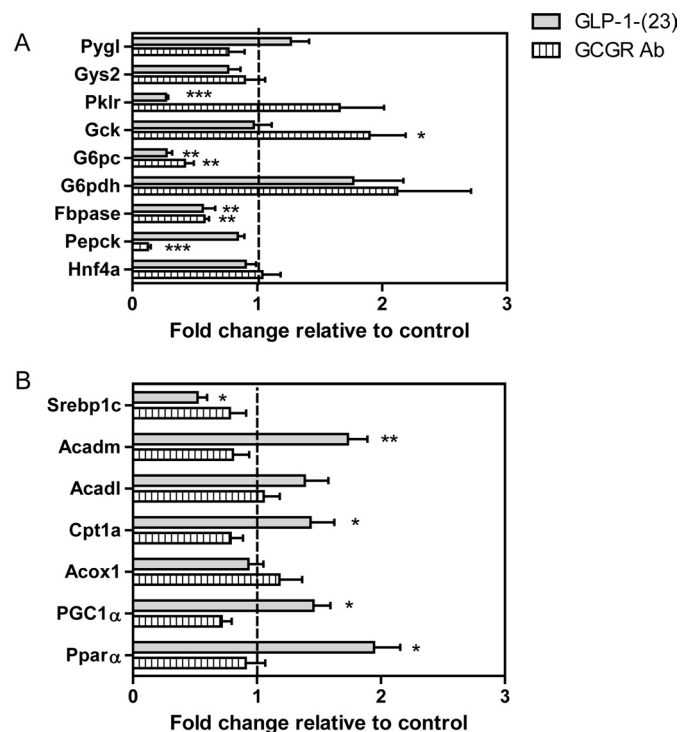


**Fig. 7.** Gene expression levels from livers of mice treated intraperitoneally with either GLP-1-(23) (filled bars) or GCGR Ab (striped bars) at doses of 10  $\mu\text{g}/\text{mouse}$  or 1  $\text{mg}/\text{kg}$ , respectively. All expression levels are shown as the fold-change relative to those of vehicle-treated control mice. A, representative glucose metabolism gene expression level changes. B, representative fatty acid metabolism gene expression level changes. \*,  $P < 0.05$ ; \*\*,  $P < 0.01$ ; \*\*\*,  $P < 0.001$  versus vehicle-treated expression levels. Pygl, phosphorylase glycogen liver; Gys2, glycogen synthase 2; Gck, glucokinase; G6pc, glucose-6-phosphatase, catalytic; Fbpase, fructose 1,6 biphosphatase; Hnf4A, hepatocyte nuclear factor 4 $\alpha$ ; Srebp1c, sterol-regulatory-element-binding protein-1c; Acadm, acyl-CoA dehydrogenase, C-4 to C-12 straight chain; Acadl, Acyl-CoA dehydrogenase, long chain; Cpt1a, carnitine palmitoyltransferase 1A; Acox1, acyl-CoA oxidase; PGC1 $\alpha$ , peroxisome proliferator-activated receptor  $\gamma$  coactivator 1 $\alpha$ ; Ppar $\alpha$ , peroxisome proliferator-activated receptor  $\alpha$ .

cagon signaling pathway leads to reduced glycemia by suppressing hepatic glucose production (Drucker and Nauck, 2006), studies have suggested that the inhibition of glucagon signaling may have additional benefits caused by an increase in circulating levels of GLP-1 (Gu et al., 2009; Yan et al., 2009). In the current studies, we investigated the different pharmacologic contributions of directly agonizing GLP-1R or antagonizing GCGR on energy state and glucose homeostasis in DIO mice.

After a single-dose administration, the GLP-1-(23)-treated mice exhibited a more robust reduction in fasting plasma glucose levels than did GCGR Ab-treated mice (Fig. 1A). The data cannot simply be explained by a reduction of glucagon activity (Fig. 1E) because both pharmacologic agents suppress the glucagon-signaling pathway. To further investigate the mechanisms of action of GLP-1-(23) and GCGR Ab, we performed a hyperglycemic clamp experiment. Consistent with the GTT data, GLP-1-(23)-treated mice displayed a greater degree of reduction of basal plasma glucose levels (12-h fast) than did GCGR Ab-treated mice (Fig. 3A). It is noteworthy that basal insulin levels were significantly increased in GLP-1-(23)-treated mice (Fig. 3B), demonstrating that during a short-term fast condition, a dose of GLP-1 is capable of stimulating insulin secretion. The superior effi-

cacy that GLP-1-(23) exhibited on basal glucose levels can be largely attributed to higher basal insulin levels observed in GLP-1-(23)-treated mice. The differential effects on insulin stimulation could be explained by greater levels of active GLP-1 in animals treated with GLP-1-(23) than in animals treated with GCGR Ab. As expected, plasma insulin levels were even higher under the hyperglycemic clamp conditions (Fig. 3B) in GLP-1-(23)-treated mice. This insulin elevation led to a greater glucose infusion rate in GLP-1-(23)-treated animals compared with that of GCGR Ab-treated mice (Fig. 3C). It is also important to state that GLP-1-(23) demonstrated higher clamped glucose levels than the other groups. Single-dose administration of the GLP-1 analog completely abolished hepatic glucose output (Fig. 3D), whereas GCGR antagonist monoclonal Ab only inhibited HGP by ~45% during the glycemic clamp. Our data are not in complete agreement with the data from Duez et al. (2009) in which exendin-4 did not completely suppress HGP. Among the factors that may contribute to the difference is that the GLP-1 analog we used is a PEGylated molecule, with a plasma half-life (>24 h) longer than that reported for exendin-4 (a few minutes). Another fact that may explain the difference between our data and that reported by Duez et al. was that exendin-4 was administered very acutely (as the euglycemic clamp is initiated) by them, whereas in our study GLP-1-(23) was given 24 h before initiating the hyperglycemic clamp. Hence, the exposure to GLP-1-(23) was longer than that of single-dose exendin-4. It is possible that this prolonged GLP-1 action led to more profound modifications of the signaling pathway involved in HGP. Finally, studies performed by Duez et al. (2009) that investigated the effects of exendin-4 used somatostatin to suppress endogenous insulin and glucagon secretion, whereas in our studies, GLP-1-(23) had profound effects on endogenous pancreatic hormone levels. The GLP-1-(23)-induced elevation of insulin levels may have contributed to the differences between the effects of GLP-1-(23) on HGP in this study versus the exendin-4 studies performed by Duez et al.

Glucagon inhibits glycolysis by reducing the levels of fructose-2,6-bisphosphate, an allosteric activator of the rate-limiting enzyme phosphofruktokinase-1 (Jiang and Zhang, 2003). The increased glycolysis exhibited by both agents is probably caused by inhibition of glucagon signaling (Fig. 4). During our clamp studies, GLP-1-(23) significantly increased the rate of glycogen synthesis, whereas GCGR Ab had no impact on this process (Fig. 4).

It is noteworthy that our results and others suggest that the glucose-lowering action of GLP-1 is in part mediated by glucose disposal via increased glycogen synthesis. Administration of GLP-1 at physiologic concentrations has been shown to increase glucose incorporation into glycogen in skeletal muscle by activating muscle glycogen synthase activity (Villanueva-Penacarrillo et al., 1994).

The GLP-1-(23) we used in the experiments is a 20-kDa PEG-peptide conjugate. Although the increased size makes the GLP-1 analog less permeable to the blood-brain barrier, we cannot exclude the possibility that a portion of the GLP-1-(23) effects may have been mediated by the central action of GLP-1 receptor. Specifically, it has been demonstrated that intracerebroventricular infusion of exendin-4 in DIO mice resulted in increased liver glycogen storage (Knauf et al., 2005). Thus the increased glycogen synthesis observed dur-

ing our clamp studies (Fig. 4) could be at least in part mediated by a central GLP-1 action. Nevertheless, it remains to be determined whether this insulin-like action is mediated by GLP-1-stimulated insulin secretion or direct action of the GLP-1 on muscle cells. Further characterization of the GLP-1 receptor expression in skeletal muscle will help elucidate the mechanisms.

The observation that GLP-1-(23) induced robust glucose uptake in brown adipose tissue (BAT) is interesting. Although the mechanisms involved are not entirely clear, several factors may contribute to the observed phenotype. First, administration of a supraphysiological dose of GLP-1 analog elevated plasma insulin levels by several-fold compared with mice treated with vehicle or GCGR Ab during the hyperglycemic clamp (Fig. 3). Insulin is known to promote glucose disposal in peripheral tissues including BAT; in fact, some rodent studies showed that BAT may be responsible for up to 20 to 25% of whole-body glucose disposal when insulin levels are elevated (Ferré et al., 1986; Holness et al., 1991). Glucose mobilized to BAT can be used or stored as fuel through glycolysis and oxidation or lipogenesis. Administration of the supraphysiological level of GLP-1 analog was accompanied with depression of food intake to the extent that mice were close to a fasting state as demonstrated by the significant decrease in RQ values. The decrease in overall energy expenditure may be explained partly by reduced physical activities (Fig. 2E). BAT is known to be responsible for thermogenic maintenance. Perhaps increased BAT thermogenesis is required for thermogenic homeostasis in mice with reduced physical activity induced by GLP-1 analog treatment. It is not known whether GLP-1R is expressed in BAT. Whether the GLP-1 action in BAT contributes significantly to the overall GLP-1 effects on glucose control and energy expenditure remains an interesting topic for future studies.

The satiety effects of GLP-1 have been well documented in both animals and humans (Näslund et al., 1999; Drucker and Nauck, 2006). It has also been reported that glucagon not only decreases food intake but also promotes lipolysis and weight loss (Day et al., 2009); therefore, GCGR antagonism may theoretically have unfavorable impacts on lipids and body weight. Thus a GCGR antagonist may have effects on energy and lipid metabolism distinct from a GLP-1 analog. As demonstrated by our current experimental data, after a single dose administered to DIO mice GLP-1-(23) displayed robust effects on food intake and body weight reduction, whereas GCGR Ab showed modest or insignificant effects on these parameters. It is interesting to note that administration of GLP-1-(23) produced a significant reduction in the RQ (Fig. 2F), suggesting increased whole-body fatty acid oxidation. Gene expression studies also showed increased transcription of peroxisome proliferator-activated receptor  $\alpha$  and peroxisome proliferator-activated receptor  $\gamma$  coactivator 1 $\alpha$ , two key regulators involved in fatty acid oxidation, only in mice treated with GLP-1-(23) (Fig. 7B). Because administration of the GLP-1 analog caused a rapid and significant reduction in food intake (Fig. 2A), the switch toward lipid metabolism suggests that these animals are in a fasting state caused by the satiety effect mediated by GLP-1 (Fig. 2A). Our data demonstrate that the GLP-1 analog has more favorable impacts on lipid and energy metabolism than the GCGR antagonist.

To delineate the effects of GLP-1 analog and GCGR Ab on the metabolic fate of  $^{13}\text{C}_1$ - $^{13}\text{C}_4$ -labeled glucose, we per-

formed SiDMAP studies in DIO mice during ipGTT. Consistent with the clamp study results, GLP-1-(23)-treated mice showed a greater degree of glucose clearance than did GCGR Ab-treated mice (Fig. 6A). Both agents suppress gene expression in the gluconeogenic pathway (Fig. 7A). In fact, GCGR Ab treatment resulted in a more robust inhibition of Pepck expression, a direct target for hepatic gluconeogenesis (Fig. 7A). This is consistent with the notion that GCGR is expressed predominantly in liver and has a direct role in transcriptional regulation of gluconeogenesis, whereas GLP-1 action on glucose output is mediated by stimulation of glycogen synthase, which is regulated primarily by post-transcriptional modifications (Jiang and Zhang, 2003; Redondo et al., 2003). Note that GLP-1-(23) treatment had no impact on the mRNA levels of glycogen synthase and glycogen phosphorylase (Fig. 7A). Although the two agents induced rapid clearance of administered tracer glucose, the metabolic fate of the labeled glucose showed both overlapping and distinct paths in mice treated with the two different antidiabetic agents. The rapid disposal of the glucose tracer by both agents was mediated by pathways including increased glycolysis and TCA cycle anaplerosis, resulting in a surge in plasma lactate and glutamate levels (Fig. 6, B and C). Both agents also increased glucose oxidation in the liver and kidney, producing ATP and carbon dioxide (Fig. 6D). GLP-1-(23) treatment uniquely exhibited increased pentose cycle flux in the liver and kidneys. This biochemical reaction yielded additional NADPH, which is required by de novo fatty acid synthesis. This is consistent with the report that GLP-1 stimulates glucose-derived de novo fatty acid synthesis during insulin release (Bulotta et al., 2003).

An important difference between GLP-1-(23) and GCGR Ab action is the difference in regulation of *Pklr* gene expression in the liver. GLP-1-(23) treatment increased  $^{13}\text{CO}_2$  and linked ATP production from glucose, which would be expected to down-regulate PKLR activity and/or expression. We observed that GCGR Ab-treated livers exhibited a slight, but insignificant, increase in *Pklr* expression in addition to glutamate  $^{13}\text{C}$  labeling significantly higher than GLP-1-(23). This is an important marker of increased anaplerosis with net production of pyruvate and oxaloacetate and is seen as increased glutamate turnover (Noguchi et al., 2009). Because GLP-1-(23) does not have such increased anaplerotic effect on liver mitochondria, the data suggest that the increase in  $^{13}\text{CO}_2$  and ATP production via complete glucose oxidation effectively down-regulates *Pklr* expression as a mitochondria-protecting mechanism.

In summary, we have conducted multiple comprehensive studies to demonstrate that two antidiabetic agents, GLP-1-(23) and GCGR Ab, exhibited overlapping and distinct mechanisms in regulating glucose homeostasis and energy metabolism.

#### Acknowledgments

We thank Scott Silbiger of Amgen Inc. for editing the manuscript.

#### Authorship Contributions

Participated in research design: Gu, Lloyd, Chinookswong, Komorowski, Winters, Boros, and Veniant.

Conducted experiments: Chinookswong, Komorowski, Sivits, Graham, and Winters.

Performed data analysis: Gu, Lloyd, Chinookswong, Komorowski, Sivits, Graham, Winters, Boros, and Veniant.

Wrote or contributed to the writing of the manuscript: Gu, Lloyd, Winters, Boros, and Veniant.

#### References

- Boros LG, Cascante M, and Lee WN (2002) Metabolic profiling of cell growth and death in cancer: applications in drug discovery. *Drug Discov Today* **7**:364–372.
- Bulotta A, Perfetti R, Hui H, and Boros LG (2003) GLP-1 stimulates glucose-derived de novo fatty acid synthesis and chain elongation during cell differentiation and insulin release. *J Lipid Res* **44**:1559–1565.
- Day JW, Ottaway N, Patterson JT, Gelfanov V, Smiley D, Gidda J, Findeisen H, Bruemmer D, Drucker DJ, Chaudhary N, et al. (2009) A new glucagon and GLP-1 co-agonist eliminates obesity in rodents. *Nat Chem Biol* **5**:749–757.
- Drucker DJ and Nauck MA (2006) The incretin system: glucagon-like peptide-1 receptor agonists and dipeptidyl peptidase-4 inhibitors in type 2 diabetes. *Lancet* **368**:1696–1705.
- Drucker DJ, Philippe J, Mojsov S, Chick WL, and Habener JF (1987) Glucagon-like peptide I stimulates insulin gene expression and increases cyclic AMP levels in a rat islet cell line. *Proc Natl Acad Sci USA* **84**:3434–3438.
- Duez H, Smith AC, Xiao C, Giacca A, Szeto L, Drucker DJ, and Lewis GF (2009) Acute dipeptidyl peptidase-4 inhibition rapidly enhances insulin-mediated suppression of endogenous glucose production in mice. *Endocrinology* **150**:56–62.
- Egan JM, Montrose-Rafizadeh C, Wang Y, Bernier M, and Roth J (1994) Glucagon-like peptide-1(7–36) amide (GLP-1) enhances insulin-stimulated glucose metabolism in 3T3–L1 adipocytes: one of several potential extrapancreatic sites of GLP-1 action. *Endocrinology* **135**:2070–2075.
- Ferré P, Burnol AF, Leturque A, Terretaz J, Penicaud L, Jeanrenaud B, and Girard J (1986) Glucose utilization in vivo and insulin-sensitivity of rat brown adipose tissue in various physiological and pathological conditions. *Biochem J* **233**:249–252.
- Flint A, Raben A, Astrup A, and Holst JJ (1998) Glucagon-like peptide 1 promotes satiety and suppresses energy intake in humans. *J Clin Invest* **101**:515–520.
- Greig NH, Holloway HW, De Ore KA, Jani D, Wang Y, Zhou J, Garant MJ, and Egan JM (1999) Once daily injection of exendin-4 to diabetic mice achieves long-term beneficial effects on blood glucose concentrations. *Diabetologia* **42**:45–50.
- Gu W, Winters KA, Motani AS, Komorowski R, Zhang Y, Liu Q, Wu X, Rulifson IC, Sivits G Jr, Graham M, et al. (2010) Glucagon receptor antagonist-mediated improvements in glycemic control are dependent on functional pancreatic GLP-1 receptor. *Am J Physiol Endocrinol Metab* **299**:E624–E632.
- Gu W, Yan H, Winters KA, Komorowski R, Vonderfecht S, Atangan L, Sivits G, Hill D, Yang J, Bi V, et al. (2009) Long-term inhibition of the glucagon receptor with a monoclonal antibody in mice causes sustained improvement in glycemic control, with reversible  $\alpha$ -cell hyperplasia and hyperglucagonemia. *J Pharmacol Exp Ther* **331**:871–881.
- Holness MJ, Liu YL, Beech JS, and Sugden MC (1991) Glucose utilization by interscapular brown adipose tissue in vivo during nutritional transitions in the rat. *Biochem J* **273**:233–235.
- Jiang G and Zhang BB (2003) Glucagon and regulation of glucose metabolism. *Am J Physiol Endocrinol Metab* **284**:E671–E678.
- Klain GJ (1977) In vivo effects of glucagon on fatty acid synthesis in fasted and re-fed rats. *J Nutr* **107**:942–948.
- Knauf C, Cani PD, Perrin C, Iglesias MA, Maury JF, Bernard E, Benhamed F, Grémeaux T, Drucker DJ, Kahn CR, et al. (2005) Brain glucagon-like peptide-1 increases insulin secretion and muscle insulin resistance to favor hepatic glycogen storage. *J Clin Invest* **115**:3554–3563.
- Lee WN, Boros LG, Puigianer J, Bassilian S, Lim S, and Cascante M (1998) Mass isotopomer study of the nonoxidative pathways of the pentose cycle with [1,2- $^{13}\text{C}$ ]glucose. *Am J Physiol Endocrinol Metab* **274**:E843–E851.
- Lee WN, Byerley LO, Bassilian S, Ajie HO, Clark I, Edmond J, and Bergner EA (1995) Isotopomer study of lipogenesis in human hepatoma cells in culture: contribution of carbon and hydrogen atoms from glucose. *Anal Biochem* **226**:100–112.
- Lee WN, Edmond J, Bassilian S, and Morrow JW (1996) Mass isotopomer study of glutamine oxidation and synthesis in primary culture of astrocytes. *Dev Neurosci* **18**:469–477.
- Leimer KR, Rice RH, and Gehrke CW (1977) Complete mass spectra of *N*-trifluoroacetyl-*n*-butyl esters of amino acids. *J Chromatogr* **141**:121–144.
- Liang Y, Osborne MC, Monia BP, Bhanot S, Gaarde WA, Reed C, She P, Jetton TL, and Demarest KT (2004) Reduction in glucagon receptor expression by an antisense oligonucleotide ameliorates diabetic syndrome in *db/db* mice. *Diabetes* **53**:410–417.
- Meeran K, O'Shea D, Edwards CM, Turton MD, Heath MM, Gunn I, Abusnana S, Rossi M, Small CJ, Goldstone AP, et al. (1999) Repeated intracerebroventricular administration of glucagon-like peptide-1(7–36) amide or exendin-(9–39) alters body weight in the rat. *Endocrinology* **140**:244–250.
- Miranda LP, Winters KA, Gegg CV, Patel A, Aral J, Long J, Zhang J, Diamond S, Guido M, Stanislaus S, et al. (2008) Design and synthesis of conformationally constrained glucagon-like peptide-1 derivatives with increased plasma stability and prolonged in vivo activity. *J Med Chem* **51**:2758–2765.
- Näslund E, Barkeling B, King N, Gutniak M, Blundell JE, Holst JJ, Rössner S, and Hellström PM (1999) Energy intake and appetite are suppressed by glucagon-like peptide-1 (GLP-1) in obese men. *Int J Obes Relat Metab Disord* **23**:304–311.
- Nauck MA, Niedereichholz U, Ettl R, Holst JJ, Orskov C, Ritzel R, and Schmiegel WH (1997) Glucagon-like peptide 1 inhibition of gastric emptying outweighs its insulinotropic effects in healthy humans. *Am J Physiol Endocrinol Metab* **273**:E981–E988.
- Noguchi Y, Young JD, Aleman JO, Hansen ME, Kelleher JK, and Stephanopoulos G (2009) Effect of anaplerotic fluxes and amino acid availability on hepatic lipooapoptosis. *J Biol Chem* **284**:33425–33436.

- Raun K, von Voss P, Gotfredsen CF, Golozoubova V, Rolin B, and Knudsen LB (2007) Liraglutide, a long-acting glucagon-like peptide-1 analog, reduces body weight and food intake in obese candy-fed rats, whereas a dipeptidyl peptidase-IV inhibitor, vildagliptin, does not. *Diabetes* **56**:8–15.
- Redondo A, Trigo MV, Acitores A, Valverde I, and Villanueva-Peñacarrillo ML (2003) Cell signalling of the GLP-1 action in rat liver. *Mol Cell Endocrinol* **204**:43–50.
- Reed WD, Baab PJ, Hawkins RL, and Ozand PT (1984) The effects of insulin and glucagon on ketone-body turnover. *Biochem J* **221**:439–444.
- Unger RH and Orci L (1975) The essential role of glucagon in the pathogenesis of diabetes mellitus. *Lancet* **1**:14–16.
- Villanueva-Peñacarrillo ML, Alcántara AI, Clemente F, Delgado E, and Valverde I (1994) Potent glycogenic effect of GLP-1(7–36)amide in rat skeletal muscle. *Diabetologia* **37**:1163–1166.
- Wahl DR, Petersen B, Warner R, Richardson BC, Glick GD, and Opipari AW (2010) Characterization of the metabolic phenotype of chronically activated lymphocytes. *Lupus* **19**:1492–1501.
- Wang Y, Perfetti R, Greig NH, Holloway HW, DeOre KA, Montrose-Rafizadeh C, Elahi D, and Egan JM (1997) Glucagon-like peptide-1 can reverse the age-related decline in glucose tolerance in rats. *J Clin Invest* **99**:2883–2889.
- Wettersgren A, Schjoldager B, Mortensen PE, Myhre J, Christiansen J, and Holst JJ (1993) Truncated GLP-1 (proglucagon 78–107-amide) inhibits gastric and pancreatic functions in man. *Dig Dis Sci* **38**:665–673.
- Xu G, Stoffers DA, Habener JF, and Bonner-Weir S (1999) Exendin-4 stimulates both  $\beta$ -cell replication and neogenesis, resulting in increased  $\beta$ -cell mass and improved glucose tolerance in diabetic rats. *Diabetes* **48**:2270–2276.
- Xu J, Lloyd DJ, Hale C, Stanislaus S, Chen M, Sivits G, Vonderfecht S, Hecht R, Li YS, Lindberg RA, et al. (2009) Fibroblast growth factor 21 reverses hepatic steatosis, increases energy expenditure, and improves insulin sensitivity in diet-induced obese mice. *Diabetes* **58**:250–259.
- Yan H, Gu W, Yang J, Bi V, Shen Y, Lee E, Winters KA, Komorowski R, Zhang C, Patel JJ, et al. (2009) Fully human monoclonal antibodies antagonizing the glucagon receptor improve glucose homeostasis in mice and monkeys. *J Pharmacol Exp Ther* **329**:102–111.
- Zander M, Madsbad S, Madsen JL, and Holst JJ (2002) Effect of 6-week course of glucagon-like peptide 1 on glycaemic control, insulin sensitivity, and  $\beta$ -cell function in type 2 diabetes: a parallel-group study. *Lancet* **359**:824–830.

---

**Address correspondence to:** Dr. Murielle Véniant, Department of Metabolic Disorders, Amgen Inc., One Amgen Center Drive, Mail Stop 29-1-A, Thousand Oaks, CA 91320. E-mail: mveniant@amgen.com

---